Bifurcation to vortex solutions in superconducting films

T. Boeck*
S.J. Chapman†
Mathematical Institute
24-29 St. Giles'
Oxford OX1 3LB

July 6, 2000

Abstract

The bifurcation from a normally conducting state to a superconducting state in a decreasing magnetic field is studied for a slab geometry. The leading eigenvalue is a double eigenvalue, leading to a rich structure of possible behaviours. A weakly-nonlinear stability analysis is performed, and the possible responses of the material are classified. Finally, the leading order equations are solved numerically for a wide range of parameter values to determine which of these behaviours will occur in practice.

1 Introduction

If a superconducting body is placed in a sufficiently strong magnetic field superconductivity will be destroyed and the body will revert to the normally conducting (normal) state. If the magnetic field is now reduced there will be a point at which the body begins to change back into the superconducting state. The way that this transformation takes place depends upon the material parameters of the superconductor (whether it is type I or type II) and the geometry of the sample. Typically, a type I superconductor will change phase by means of phase boundaries separating superconducting material from normal material sweeping through the sample. For type II superconductors the phase change is more gradual, with the superconductor first forming a mixed state in which both normal

*Present address: Institute of Aerospace Engineering, Dresden University of Technology,01062 Dresden,Germany

†Supported by a Nuclear Electric Research Fellowship

and superconducting regions are present. In the mixed state the normal material is distributed in thin filaments, each carrying a quantised amount of magnetic flux, and circled by a vortex of superconducting current.

The bifurcation from the normal state to a superconducting state in a decreasing magnetic field was first considered by Ginzburg & Landau [10] for an infinite superconducting domain, and by Saint-James and de Gennes [17] for a halfspace. Since then it has been extensively studied in both the physics and mathematics literature, see for example [2, 3, 4, 7, 12, 13, 15, 18]. For a superconductor occupying the whole of space it is found that the bifurcation is subcritical for type I superconductors but supercritical for type II superconductors; hence the observation of the mixed state only for type II superconductors. Furthermore, for a superconducting halfspace it was found that the field at which the bifurcation occurs was higher than that for the superconductor occupying the whole space, with the superconducting solution being localised near the boundary of the domain. Thus superconductivity will nucleate first on the surface of a body, a phenomenon known as surface superconductivity. Again there were regions of parameter space corresponding to sub- and supercritical bifurcations, although the switch between the two was now not in the same place as before.

The bifurcation for an arbitrary domain was developed in [3, 4, 13] assuming that the relevant eigenvalue was simple; this is indeed the case for the halfspace and wholespace examples considered. However, if we consider a large but finite superconducting slab, then presumably it will resemble a halfspace in coordinates fixed at either end, so that the leading eigenvalue will have two eigenfunctions: one localised on the left boundary and one localised on the right boundary.

The aim of the present paper is to consider this double eigenvalue problem, generalising the results of [3, 4].

In Section 2 we examine the steady state problem. We will find that there are three superconducting solution branches coming from the bifurcation point corresponding to surface superconductivity on the left boundary, on the right boundary, and on both boundaries respectively. The interference produced when both eigenfunctions are present produces a row of zeros down the centre of the slab, corresponding to the vortices of the mixed state.

It is then of interest to determine which of these solutions, if any, will be observed in practice. We look at the time-dependent problem via a weakly-nonlinear stability analysis in Section 3.

Finally, in Section 4, we present our conclusions.

2 Superconductivity in a Thin Film in a Parallel Magnetic Field

2.1 Ginzburg–Landau equations

We consider a superconducting film of thickness $2d$ which occupies the region $-d < x < d$ and is infinite in the y– and z–directions.

The film is held at constant temperature and is placed in an homogeneous magnetic field of strength h pointing in z–direction. The non–dimensionalized Ginzburg–Landau equations and boundary conditions for this problem read [5, 9, 10]

$$
\begin{aligned}
\left((i/\kappa)\nabla + \mathbf{A}\right)^2 \Psi &= \Psi\left(1 - |\Psi|^2\right) \quad \text{in } |x| < d, && (1)\\
-\nabla \times (\nabla \times \mathbf{A}) &= \frac{i}{2\kappa}\left(\Psi^*\nabla\Psi - \Psi\nabla\Psi^*\right) + |\Psi|^2 \mathbf{A} \quad \text{in } |x| < d, && (2)\\
-\nabla \times (\nabla \times \mathbf{A}) &= \mathbf{0} \quad \text{in } |x| > d, && (3)\\
\mathbf{n} \cdot \left((i/\kappa)\nabla + \mathbf{A}\right)\Psi &= -(i/D)\Psi \quad \text{on } |x| = d, && (4)\\
[\mathbf{n} \times \mathbf{A}] &= \mathbf{0}, && (5)\\
[\mathbf{n} \times (1/\mu)\nabla \times \mathbf{A}] &= \mathbf{0}, && (6)\\
\nabla \times \mathbf{A} &\to h\mathbf{e}_z \quad \text{as } |x| \to \infty. && (7)
\end{aligned}
$$

Here Ψ is the complex order parameter, such that $|\Psi|^2$ represents the number density of the superconducting charge carriers, $\mathbf{A}$ is the magnetic vector potential (such that $\mathbf{H} = \nabla \times \mathbf{A}$ is the magnetic field), $\mathbf{e}_z$ is the unit vector in z-direction, and $\mathbf{n}$ stands for the outward normal vector. The brackets [ ] denote the jump in the enclosed quantity across the boundary of the film, and $*$ stands for complex conjugation. The constant μ is the permeability, and κ is the Ginzburg–Landau parameter, which determines the type of superconductor; materials with $\kappa < 1/\sqrt{2}$ are known as type I superconductors, while those with $\kappa > 1/\sqrt{2}$ are known as type II superconductors. It is assumed that there are no currents outside the superconductor, so that the vector potential outside the film is given by (3). The boundary conditions (5) and (6) are the usual conditions on $\mathbf{A}$ at the interface between different magnetic media. Equation (7) states that the magnetic field reduces to the applied field at large distances from the film.

The boundary condition (4) is due to de Gennes [8]. The parameter D depends on the material adjacent to the superconductor, and can range from 0 (for the case of an adjacent magnetic material) to ∞ (for an adjacent insulator).

Equations (1)–(7) are gauge–invariant in the sense that if $(\Psi, \mathbf{A})$ is a solution then the transformed functions $(e^{i\kappa\eta}\Psi, \mathbf{A} + \nabla\eta)$ will also be a solution for an arbitrary scalar function η. This property means that extra conditions need to be imposed (known as gauge conditions) in order to make the solution to (1)–(7) unique. However, physical quantities such as the magnetic field and the modulus of Ψ are not affected by a gauge transform. We will make use of the gauge–invariance by choosing a simple expression for $\mathbf{A}$ as we proceed with the calculations.

2.2 Perturbation Solution

The solution of (1)–(7) corresponding to the normal state is

$$\Psi \equiv 0, \qquad \mathbf{A} = h\mathbf{A}_N. \tag{8}$$

where $\mathbf{A}_N$ satisfies the equations

$$\begin{aligned}
\nabla \times (\nabla \times \mathbf{A}_N) &= \mathbf{0} \quad \text{except on } |x| = d, & (9)\\
[\mathbf{n} \times \mathbf{A}_N] &= \mathbf{0}, & (10)\\
[\mathbf{n} \times (1/\mu)\,\nabla \times \mathbf{A}_N] &= \mathbf{0}, & (11)\\
\nabla \times \mathbf{A}_N &\to \mathbf{e}_z \quad \text{as } |x| \to \infty. & (12)
\end{aligned}$$

We now apply a perturbation procedure introduced in [13] and described in more detail in [3] to the equations (1)–(7). Let

$$\begin{aligned}
\Psi &= \epsilon^{1/2}\psi, & (13)\\
\mathbf{A} &= h\mathbf{A}_N + \epsilon\mathbf{a}, & (14)
\end{aligned}$$

where $\epsilon \ll 1$ is introduced as a measure of the size of $|\Psi|^2$. Now h, $\mathbf{a}$ and ψ are expanded in ϵ:

$$\begin{aligned}
h &= h^{(0)} + \epsilon h^{(1)} + \cdots, & (15)\\
\mathbf{a} &= \mathbf{a}^{(0)} + \epsilon\mathbf{a}^{(1)} + \cdots, & (16)\\
\psi &= \psi^{(0)} + \epsilon\psi^{(1)} + \cdots. & (17)
\end{aligned}$$

Inserting these expansions and (13), (14) into (1)–(7) gives the leading order problem

$$\begin{aligned}
\left((i/\kappa)\,\nabla + h^{(0)}\mathbf{A}_N\right)^2 \psi^{(0)} - \psi^{(0)} &= 0 \quad \text{in } |x| < d, & (18)\\
-\nabla \times \left(\nabla \times \mathbf{a}^{(0)}\right) &= (i/2\kappa)\left(\psi^{(0)*}\nabla\psi^{(0)} - \psi^{(0)}\nabla\psi^{(0)*}\right) & \\
&\quad + h^{(0)}\left|\psi^{(0)}\right|^2 \mathbf{A}_N \quad \text{in } |x| < d, & (19)\\
-\nabla \times \left(\nabla \times \mathbf{a}^{(0)}\right) &= \mathbf{0} \quad |x| > d, & (20)\\
\mathbf{n} \cdot \left((i/\kappa)\,\nabla + h^{(0)}\mathbf{A}_N\right)\psi^{(0)} &= -\,(i/D)\,\psi^{(0)} \quad \text{on } |x| = d, & (21)\\
\left[\mathbf{n} \times \mathbf{a}^{(0)}\right] &= \mathbf{0}, & (22)\\
\left[\mathbf{n} \times (1/\mu)\,\nabla \times \mathbf{a}^{(0)}\right] &= \mathbf{0}, & (23)\\
\nabla \times \mathbf{a}^{(0)} &\to \mathbf{0} \quad \text{as } |x| \to \infty. & (24)
\end{aligned}$$

Equation (18) and the boundary condition (21) represent an eigenvalue problem for $h^{(0)}$. The upper critical field h_{c_3} is defined as the largest eigenvalue.

Since the equation for $\psi^{(0)}$ is linear, $\psi^{(0)}$ can only be determined up to a factor. If the eigenvalue h_{c_3} is degenerate, then the coefficients in a linear combination of all the eigenfunctions corresponding to h_{c_3} are unknown. We need to consider the equations for $\psi^{(1)}$ and $\mathbf{a}^{(1)}$ in order to find them. These equations are

$$\begin{aligned}
&\left((i/\kappa)\nabla + h^{(0)}\mathbf{A}_N\right)^2 \psi^{(1)} - \psi^{(1)} = -\psi^{(0)}\left|\psi^{(0)}\right|^2 - 2h^{(1)}h^{(0)}\left|\mathbf{A}_N\right|^2\psi^{(0)} \\
&-2h^{(1)}(i/\kappa)\left(\mathbf{A}_N\cdot\nabla\psi^{(0)}\right) - 2(i/\kappa)\left(\mathbf{a}^{(0)}\cdot\nabla\psi^{(0)}\right) - (i/\kappa)\psi^{(0)}\nabla\cdot\mathbf{a}^{(0)} \\
&-(i/\kappa)h^{(1)}\psi^{(0)}\nabla\cdot\mathbf{A}_N - 2h^{(0)}\psi^{(0)}\left(\mathbf{A}_N\cdot\mathbf{a}^{(0)}\right) \quad \text{in } |x| < d, \qquad (25)
\end{aligned}$$

$$\begin{aligned}
&-\nabla\times\left(\nabla\times\mathbf{a}^{(1)}\right) = (i/2\kappa)\left(\psi^{(0)*}\nabla\psi^{(1)} + \psi^{(1)*}\nabla\psi^{(0)}\right) \\
&-(i/2\kappa)\left(\psi^{(0)}\nabla\psi^{(1)*} + \psi^{(1)}\nabla\psi^{(0)*}\right) + h^{(0)}\mathbf{A}_N\left(\psi^{(0)}\psi^{(1)*} + \psi^{(1)}\psi^{(0)*}\right) \\
&+h^{(1)}\left|\psi^{(0)}\right|^2\mathbf{A}_N + \left|\psi^{(0)}\right|^2\mathbf{a}^{(0)} \quad \text{in } |x| < d, \qquad (26)
\end{aligned}$$

$$\begin{aligned}
-\nabla\times\left(\nabla\times\mathbf{a}^{(1)}\right) &= \mathbf{0} \quad |x| > d, & (27)\\
\mathbf{n}\cdot\left((i/\kappa)\nabla + h^{(0)}\mathbf{A}_N\right)\psi^{(1)} + (i/D)\psi^{(1)} &= -\mathbf{n}\cdot\left(\mathbf{a}^{(0)} + h^{(1)}\mathbf{A}_N\right)\psi^{(0)} \\
&\quad\ \text{on } |x| = d, & (28)\\
\left[\mathbf{n}\times\mathbf{a}^{(1)}\right] &= \mathbf{0}, & (29)\\
\left[\mathbf{n}\times(1/\mu)\nabla\times\mathbf{a}^{(1)}\right] &= \mathbf{0}, & (30)\\
\nabla\times\mathbf{a}^{(1)} &\to \mathbf{0} \quad \text{as } |x|\to\infty. & (31)
\end{aligned}$$

Equations (25) and (28) are inhomogeneous versions of (18) and (21) and have solutions if and only if their right hand sides satisfy certain solvability conditions. These solvability conditions will allow us to determine $\psi^{(0)}$ completely.

At this point we impose our gauge constraints. We seek a solution in which the physical quantities $\mathbf{H}$ and $|\Psi|^2$ are funcions of x only. Hence we can choose as a gauge $\mathbf{A} = (0, A(x), 0)$. However, even this does not determine A uniquely, since any constant could be added to A without affecting $\mathbf{H}$. Thus, to fix the gauge we impose the additional constraint that $A(0) = 0$.

We now turn to the solution of the leading order equations. With $\mathbf{A}_N = (0, A_N(x), 0)$, (9)–(12) imply

$$\frac{d^2 A_N}{dx^2} = 0, \qquad (32)$$

with $dA_N/dx \to 1$ as $|x| \to \infty$, and A_N and dA_N/dx continuous at $|x| = d$.Thus, $A_N(x) = x$.

Equation (18) has solutions

$$\psi^{(0)}(x, y, z) = f(x)e^{-i(k_y y + k_z z)}, \qquad (33)$$

as observed in [18], where it is also pointed out that the maximum eigenvalue $h^{(0)}$ occurs for $k_z = 0$. This can easily be shown using the calculus of variations.

We therefore restrict ourselves to solutions of the form

$$\psi^{(0)}(x,y) = f(x)e^{-ih^{(0)}\kappa c y} \tag{34}$$

and linear combinations of such solutions for the case of a degenerate eigenvalue $h^{(0)}$. The exponential in (34) has been chosen so that the following equations take a simple form.

Inserting (34) into (18)–(24), with $\mathbf{a} = (0, a, 0)$, we find

$$\begin{aligned} \kappa^{-2} f'' &= -f + \left(h^{(0)}\right)^2 (x+c)^2 f^{(0)}, & (35)\\ a^{(0)\prime\prime} &= h^{(0)} (x+c) f^2, & (36)\\ f'(-d) = (\kappa/D) f(-d), &\qquad f'(d) = -(\kappa/D) f(d), & (37)\\ a^{(0)\prime}(-d) = 0, &\qquad a^{(0)\prime}(d) = 0, & (38) \end{aligned}$$

where $'$ denotes d/dx.

The equation (35) together with the boundary conditions (37) represents an eigenvalue problem for $h^{(0)}$ with c as a parameter. In the following, we will always consider $h^{(0)}$ to be the largest eigenvalue of (35). The upper critical field is the maximum of $h^{(0)}(c)$, which is attained for $c = c_{max}$.

Integrating (36) from $-d$ to d and applying (38) gives the condition

$$\int_{-d}^{d} f^2(x)\,(x+c)\,dx = 0, \tag{39}$$

which must hold for (36), (38) to have a solution. Kulik has shown that (39) holds automatically if $h^{(0)}(c)$ is maximal, i.e. for $c = c_{max}$ [12].

If $c_{max} \neq 0$, there exists a second solution of the form (34) corresponding to the upper critical field, namely

$$f(-x)e^{ih^{(0)}\kappa c y}. \tag{40}$$

The solution $\psi^{(0)}$ of the leading order equation (18) then becomes a linear combination

$$\psi^{(0)} = a f(x) e^{-ih^{(0)}\kappa c y} + b f(-x) e^{ih^{(0)}\kappa c y} \tag{41}$$

with coefficients a and b which follow from solvability conditions for equation (25). These conditions have also been derived in [12]. We outline the calculation here because it is essentially the same as in the time–dependent case.

For the evaluation of the right hand side of (25) the correction $\mathbf{a}^{(0)}$ to the vector potential must be known. We denote by $a_+(x)$ a solution of (36) for $f(x)$,

$c = c_{max}$ and by $a_-(x)$ a solution of (36) for $f(-x)$, $c = -c_{max}$. Inserting the ansatz (41) into (19) gives

$$
\begin{aligned}
-\left(\mathrm{curl}\right)^2 \mathbf{a}^{(0)} = \mathbf{e}_x &\left\{ \frac{i}{2\kappa}\left[f(-x)f'(x) + f(x)f'(-x)\right]\left(ab^* e^{-2ih^{(0)}\kappa c y} - a^* b e^{2ih^{(0)}\kappa c y}\right)\right\} \\
&+ \mathbf{e}_y \left\{ |a|^2 f^2(x) h^{(0)}\left(x + c\right) + |b|^2 f^2(-x) h^{(0)}\left(x - c\right) \right. \\
&\left. + f(x)f(-x)h^{(0)}x\left(ab^* e^{-2ih^{(0)}\kappa c y} + a^* b e^{2ih^{(0)}\kappa c y}\right)\right\}. \qquad (42)
\end{aligned}
$$

A solution $\mathbf{a}^{(0)} = (0, a^{(0)}(x, y), 0)$ is therefore given by

$$
a^{(0)} = \frac{I(x)}{4\kappa^2 h^{(0)} c}\left(ab^* e^{-2ih^{(0)}\kappa c y} + a^* b e^{2ih^{(0)}\kappa c y}\right) + |a|^2 a_+(x) + |b|^2 a_-(x), \qquad (43)
$$

where the function I stands for

$$
I(x) = \int_{-d}^{x} \left(f(-\tilde{x})f'(\tilde{x}) + f(\tilde{x})f'(-\tilde{x})\right) d\tilde{x}. \qquad (44)
$$

Its derivatives are given by

$$
\begin{aligned}
I'(x) &= f(-x)f'(x) + f(x)f'(-x), & (45) \\
I''(x) &= 4\kappa^2 \left(h^{(0)}\right)^2 c x f(x) f(-x), & (46)
\end{aligned}
$$

where equation (35) has been used. From the boundary condition (37) it follows that $I'(-d) = I'(d) = 0$.

With this result equation (25) becomes

$$
\begin{aligned}
&\left(\left(i/\kappa\right)\nabla + h^{(0)}\mathbf{A}_N\right)^2 \psi^{(1)} - \psi^{(1)} = \\
&= e^{ih^{(0)}\kappa c y}\Big\{ - b|b|^2 f^3(-x) - 2b|a|^2 f^2(x) f(-x) - 2b|a|^2 \frac{I f(x) x}{4\kappa^2 c} \\
&\qquad - 2bh^{(0)}\left(x - c\right) f(-x)\left[h^{(1)}x + |a|^2 a_+ + |b|^2 a_-\right]\Big\} \\
&+ e^{-ih^{(0)}\kappa c y}\Big\{ - a|a|^2 f^3(x) - 2a|b|^2 f^2(-x) f(x) - 2a|b|^2 \frac{I f(-x) x}{4\kappa^2 c} \\
&\qquad - 2ah^{(0)}\left(x + c\right) f(x)\left[h^{(1)}x + |a|^2 a_+ + |b|^2 a_-\right]\Big\} \\
&+ e^{3ih^{(0)}\kappa c y}\Big\{ - a^* b^2 f^2(-x) f(x) - 2a^* b^2 \frac{I f(-x)}{4\kappa^2 c}\left(x - 2c\right)\Big\} \\
&+ e^{-3ih^{(0)}\kappa c y}\Big\{ - b^* a^2 f^2(x) f(-x) - 2b^* a^2 \frac{I f(x)}{4\kappa^2 c}\left(x + 2c\right)\Big\}. \qquad (47)
\end{aligned}
$$

Since $f(x)e^{-ih^{(0)}\kappa c y}$ and $f(-x)e^{ih^{(0)}\kappa c y}$ are non–trivial solutions of the homogeneous equation, the rhs of (47) must be orthogonal to the solutions of the adjoint equation. These solutions are $f(x)e^{ih^{(0)}\kappa cy}$ and $f(-x)e^{-ih^{(0)}\kappa cy}$. They give the solvability conditions

$$\begin{aligned} a\left(P|a|^2+Q|b|^2+h^{(1)}R\right) &= 0, && (48)\\ b\left(P|b|^2+Q|a|^2+h^{(1)}R\right) &= 0, && (49)\end{aligned}$$

where the quantities P, Q and R are given by

$$\begin{aligned} P &= \int_{-d}^{d}\left(-f^4(x)+2\left(a_+'\right)^2\right)dx=\int_{-d}^{d}\left(-f^4(-x)+2\left(a_-'\right)^2\right)dx, && (50)\\ Q &= 2\int_{-d}^{d}\left(-f^2(x)f^2(-x)+a_+'a_-'+\frac{I'I'}{(4\kappa^2h^{(0)}c)^2}\right)dx, && (51)\\ R &= \int_{-d}^{d}a_+'dx=\int_{-d}^{d}a_-'dx=-\int_{-d}^{d}xa_+''dx. && (52)\end{aligned}$$

The system (48), (49) has solutions

$$|a|^2=\frac{-h^{(1)}R}{P},\quad b=0\quad\text{(left boundary state)},\qquad (53)$$

$$a=0,\quad |b|^2=\frac{-h^{(1)}R}{P}\quad\text{(right boundary state)},\qquad (54)$$

$$|a|^2=|b|^2=\frac{-h^{(1)}R}{P+Q}\quad\text{(symmetric state)},\qquad (55)$$

providing $h^{(1)}$ has the proper sign. The trivial solution $a=b=0$ is always possible. In the distinction between left and right boundary states we have adopted the convention $c>0$. If $P=Q$, then only $|a|^2+|b|^2$ is determined by (48), (49).

Note that for the solution given by (55) (with a, b real and positive) we have

$$\begin{aligned} \psi^{(0)} &= \left(-\frac{h^{(1)}R}{P+Q}\right)^{1/2}\left(f(x)e^{-ih^{(0)}\kappa cy}+f(-x)e^{ih^{(0)}\kappa cy}\right), && (56)\\ &= \left(-\frac{h^{(1)}R}{P+Q}\right)^{1/2}\Big((f(x)+f(-x))\cos(h^{(0)}\kappa cy)\\ &\qquad +i(f(x)-f(-x))\sin(h^{(0)}\kappa cy)\Big), && (57)\end{aligned}$$

so that $|\psi^{(0)}|^2$ has a line of zeros at $x=0$, $y=(n+1/2)\pi/(h^{(0)}\kappa c)$, as shown in Figure 1. Each of these zeros corresponds to a supercurrent vortex.

3 Weakly–nonlinear Stability of the Normal State

3.1 Time–dependent Ginzburg–Landau equations

We now investigate the stability of these solutions by means of a weakly–nonlinear analysis near the critical field. To this end we consider the time–dependent generalisation of the Ginzburg–Landau equations due to Gorkov and Eliashberg [11]. The non–dimensionalised equations for the film problem read [4]

$$\frac{\alpha}{\kappa^2}\frac{\partial \Psi}{\partial t} + \frac{i\alpha}{\kappa}\Psi\Phi + \left(\frac{i}{\kappa}\nabla + \mathbf{A}\right)^2 \Psi = \Psi\left(1 - |\Psi|^2\right) \quad \text{in } |x| < d, \tag{58}$$

$$-\nabla \times (\nabla \times \mathbf{A}) - \frac{\partial \mathbf{A}}{\partial t} - \nabla\Phi = \frac{i}{2\kappa}\left(\Psi^*\nabla\Psi - \Psi\nabla\Psi^*\right) + |\Psi|^2\,\mathbf{A} \quad \text{in } |x| < d, \tag{59}$$

$$-\nabla \times (\nabla \times \mathbf{A}) = \varsigma_e\left(\frac{\partial \mathbf{A}}{\partial t} + \nabla\Phi\right) \quad \text{in } |x| > d, \tag{60}$$

$$\nabla^2\Phi = 0 \quad \text{in} |x| > d, \tag{61}$$

$$2\mathbf{n}\cdot\left(\left(i/\kappa\right)\nabla + \mathbf{A}\right)\Psi = -(i/D)\Psi \quad \text{on } |x| = d, \tag{62}$$

$$[\mathbf{n} \times \mathbf{A}] = \mathbf{0}, \tag{63}$$

$$[\mathbf{n} \times (1/\mu)\,\nabla \times \mathbf{A}] = \mathbf{0}, \tag{64}$$

$$[\Phi] = 0, \tag{65}$$

$$\left[\varepsilon\frac{\partial \Phi}{\partial n}\right] = 0, \tag{66}$$

$$\Phi \to 0 \quad \text{as } |x| \to \infty, \tag{67}$$

$$\nabla \times \mathbf{A} \to h\mathbf{e}_z \quad \text{as } |x| \to \infty. \tag{68}$$

In addition to the magnetic vector potential the electric potential Φ enters these equations. The constant ε is the relative permittivity, ς_e is the conductivity of the external region, scaled with the conductivity of the superconducting region in the normal state, and α is a material parameter determining the relaxation rate of the order parameter. Equation (60) is the Maxwell equation that relates the current density with the magnetic field. It is assumed that the current density outside the superconductor is given by Ohm's law. It is also assumed that there are no electric charges in the outside region, hence the right hand side of the Maxwell equation (61) is zero. The boundary conditions (65) and (66) for Φ state that the electric field remains finite at the boundary and that there is no surface charge. The boundary conditions on Ψ and $\mathbf{A}$ remain unchanged. Equations (67) and (68) state that both the electric and the magnetic fields reduce to the applied fields at large distances from the film.

3.2 Perturbation Solution

In order to examine the stability near the critical field we follow the procedure in [4] and let

$$h = h^{(0)} + \epsilon h^{(1)}. \tag{69}$$

The scalings for Ψ, $\mathbf{A}$ and ϕ are

$$\Psi = \epsilon^{1/2}\psi, \tag{70}$$

$$
\begin{aligned}
\mathbf{A} &= h\mathbf{A}_N + \epsilon \mathbf{a}, && (71)\\
\Phi &= \epsilon\phi. && (72)
\end{aligned}
$$

Linear stability analyses near the critical field show that all modes either decay exponentially on a timescale of $O(1)$, or decay or grow exponentially on a timescale of $O(1/\epsilon)$ [4]. For times of $O(1/\epsilon)$ all the modes decaying on the $O(1)$–timescale can be neglected. We can therefore treat the timescales separately.

Short Timescale: $t = O(1)$. The short–time solution is denoted by $\psi_s(\mathbf{r},t)$, $\mathbf{a}_s(\mathbf{r},t)$, $\phi_s(\mathbf{r},t)$, and is expanded in powers of ϵ:

$$
\begin{aligned}
\psi_s &= \psi_s^{(0)} + \epsilon\psi_s^{(1)} + \cdots, && (73)\\
\mathbf{a}_s &= \mathbf{a}_s^{(0)} + \epsilon\mathbf{a}_s^{(1)} + \cdots, && (74)\\
\phi_s &= \phi_s^{(0)} + \epsilon\phi_s^{(1)} + \cdots. && (75)
\end{aligned}
$$

The leading order equations take the form

$$
\begin{aligned}
\frac{\alpha}{\kappa^2}\frac{\partial\psi_s^{(0)}}{\partial t} + \left(\frac{i}{\kappa}\nabla + h^{(0)}\mathbf{A}_N\right)^2\psi_s^{(0)} &= \psi_s^{(0)} \quad \text{in } |x|<d, && (76)\\
-\nabla\times\left(\nabla\times\mathbf{a}_s^{(0)}\right) - \frac{\partial\mathbf{a}_s^{(0)}}{\partial t} - \nabla\phi_s^{(0)} &= (i/2\kappa)\left(\psi_s^{(0)*}\nabla\psi_s^{(0)} - \psi_s^{(0)}\nabla\psi_s^{(0)*}\right)\\
&\quad + h^{(0)}\left|\psi_s^{(0)}\right|^2\mathbf{A}_N \quad \text{in } |x|<d, && (77)\\
-\nabla\times\left(\nabla\times\mathbf{a}_s^{(0)}\right) &= \varsigma_e\left(\frac{\partial\mathbf{a}_s^{(0)}}{\partial t} + \nabla\phi_s^{(0)}\right) \text{ in } |x|>d, && (78)\\
\nabla^2\psi_s^{(0)} &= 0 \quad \text{in } |x|>d, && (79)\\
\mathbf{n}\cdot\left(\left(i/\kappa\right)\nabla + h^{(0)}\mathbf{A}_N\right)\psi_s^{(0)} &= -\left(i/D\right)\psi_s^{(0)} \quad \text{on } |x|=d, && (80)
\end{aligned}
$$

with $\mathbf{a}_s^{(0)}$, $\phi_s^{(0)}$ satisfying (63)–(68).

We seek solutions to (76) and (80) for the thin film problem which are independent of z and periodic in y with period $2\pi/(h^{(0)}\kappa c)$. Substituting the ansatz

$$
\psi_s^{(0)} = f(x,t)e^{ih^{(0)}\kappa n c y}, \qquad (81)
$$

(n integer) into equations (76) and (80) gives the problem

$$
\begin{aligned}
-\frac{1}{\kappa^2}f_{xx} + \left(h^{(0)}\right)^2(x-nc)^2 f - f &= -\frac{\alpha}{\kappa^2}f_t, && (82)\\
f_x(-d,t) = \frac{\kappa}{D}f(-d,t), \qquad f_x(d,t) &= -\frac{\kappa}{D}f(d,t), && (83)
\end{aligned}
$$

which has the solution

$$
f(x,t) = \sum_{k=0}^{\infty} C_k\Theta_k(x)e^{\sigma_k t}. \qquad (84)
$$

Here σ_k are the eigenvalues and Θ_k are the eigenfunctions of

$$-\frac{1}{\kappa^2}\Theta'' + \left[\left(h^{(0)}\right)^2 (x-nc)^2 - 1\right]\Theta = -\frac{\alpha\sigma}{\kappa^2}\Theta, \tag{85}$$

$$\Theta'(-d) = \frac{\kappa}{D}\Theta(-d), \qquad \Theta'(d) = -\frac{\kappa}{D}\Theta(d). \tag{86}$$

Consequently, we can write the solution to (76) and (80) as

$$\psi_s^{(0)}(x,y,t) = \sum_{n=-\infty}^{\infty}\sum_{k=0}^{\infty} C_{n,k}\Theta_{n,k}(x)e^{ih^{(0)}\kappa ncy}e^{\sigma_{n,k}t}, \tag{87}$$

where the coefficients $C_{n,k}$ are determined by the initial condition

$$\psi_s^{(0)}(x,y,0) = \sum_{n=-\infty}^{\infty}\sum_{k=0}^{\infty} C_{n,k}\Theta_{n,k}(x)e^{ih^{(0)}\kappa ncy}. \tag{88}$$

The eigenvalues $\sigma_{n,k}$ are all less than or equal to zero. To demonstrate this, note that equation (85) has the eigenvalue $\sigma = 0$ for $n = 1$ or $n = -1$ because of (35). For any other n, let $(h_n^{(0)})^2$ denote the largest eigenvalue for $\tilde{c} = nc$ in (35). Since $(h^{(0)})^2$ is maximal, $(h_n^{(0)})^2$ is smaller than $(h^{(0)})^2$, and we obtain

$$-\frac{1}{\kappa^2}\Theta'' + \left[(h_n^{(0)})^2(x-\tilde{c})^2 + \delta(x) - 1\right]\Theta = -\frac{\alpha\sigma}{\kappa^2}\Theta, \tag{89}$$

$$\delta(x) = \left[(h^{(0)})^2 - (h_n^{(0)})^2\right](x-\tilde{c})^2 \geq 0, \tag{90}$$

where δ can be considered as a change in the function multiplying Θ. For $\delta = 0$ the largest eigenvalue will be $\sigma = 0$ by the same argument as for $|n| = 1$.

Now we can make use of theorem 7 on p.411 in [6] to conclude that a positive δ gives rise to a non–positive change in all eigenvalues σ_k of (89). Therefore, we may assume that the $\sigma_{n,k}$ are negative for all n and k except for $|n| = 1$, $k = 0$, where $\sigma_{n,0} = 0$.

Consequently, the solution tends to

$$\psi_s^{(0)} = C_{1,0}\Theta_{1,0}e^{ih^{(0)}\kappa cy} + C_{-1,0}\Theta_{-1,0}e^{-ih^{(0)}\kappa cy} \tag{91}$$

as $t \to \infty$. The leading–order solution does not exhibit a growth or decay on a $O(1)$–timescale. Note that the result (91) agrees with (41).

Long Timescale: $t = O(1/\epsilon)$.

Following [4] we put

$$\tau = \epsilon t \tag{92}$$

and consider τ to be $O(1)$. We denote the solution on the long timescale by $\psi_l(\mathbf{r},\tau)$, $\mathbf{a}_l(\mathbf{r},\tau)$, $\phi_l(\mathbf{r},\tau)$, and expand in ϵ as before:

$$\psi_l = \psi_l^{(0)} + \epsilon\psi_l^{(1)} + \cdots, \tag{93}$$

$$\mathbf{a}_l = \mathbf{a}_l^{(0)} + \epsilon\mathbf{a}_l^{(1)} + \cdots, \tag{94}$$

$$\phi_l = \phi_l^{(0)} + \epsilon\phi_l^{(1)} + \cdots. \tag{95}$$

Substituting these expansions into (58)–(68) and introducing τ gives at leading order

$$\begin{aligned}
\left((i/\kappa)\nabla + h^{(0)}\mathbf{A}_N\right)^2 \psi_l^{(0)} - \psi_l^{(0)} &= 0 \quad \text{in } |x|<d, && (96)\\
-\nabla\times\left(\nabla\times\mathbf{a}_l^{(0)}\right) - \nabla^2\phi_l^{(0)} &= (i/2\kappa)\left(\psi_l^{(0)*}\nabla\psi_l^{(0)} - \psi_l^{(0)}\nabla\psi_l^{(0)*}\right) \\
&\quad + h^{(0)}\left|\psi_l^{(0)}\right|^2 \mathbf{A}_N \quad \text{in } |x|<d, && (97)\\
-\nabla\times\left(\nabla\times\mathbf{a}_l^{(0)}\right) &= \varsigma_e\nabla\phi_l^{(0)} \quad \text{in } |x|>d, && (98)\\
\nabla^2\phi_l^{(0)} &= 0 \quad \text{in } |x|>d, && (99)\\
\mathbf{n}\cdot\left((i/\kappa)\nabla + h^{(0)}\mathbf{A}_N\right)\psi_l^{(0)} &= -(i/D)\,\psi_l^{(0)} \quad \text{on } |x|=d, && (100)
\end{aligned}$$

with $\mathbf{a}_l^{(0)}$ and $\phi_l^{(0)}$ satisfying (63)–(68). Equations (96) and (100) are exactly equations (18) and (21), and have therefore the solution (41). The coefficients are now time–dependent:

$$\psi_l^{(0)} = a(\tau)f(x)e^{-ih^{(0)}\kappa c y} + b(\tau)f(-x)e^{ih^{(0)}\kappa c y}. \tag{101}$$

Substituting this result into (97) gives

$$-\nabla\times\left(\nabla\times\mathbf{a}_l^{(0)}\right) - \nabla\phi_l^{(0)} = -\nabla\times\left(\nabla\times\mathbf{a}^{(0)}\right) \quad \text{in } \Omega, \tag{102}$$

with $\text{curl}^2\mathbf{a}^{(0)}$ as in (42). By taking the divergence of this equation we get

$$\nabla^2\phi_l^{(0)} = 0 \quad \text{in } |x|<d, \tag{103}$$

hence $\nabla^2\phi_l^{(0)}(x,y,\tau) = 0$ everywhere, except on $|x| = d$. This, together with the boundary conditions (65), (66) and (67) implies

$$\phi_l^{(0)}(x,y,\tau) \equiv 0. \tag{104}$$

Therefore equations (97) and (98) again have the solution (43).

As in the time–independent case, the coefficients $a(\tau)$, $b(\tau)$ are obtained from certain solvability conditions for the equations determining $\psi_l^{(1)}$. These equations now read

$$\begin{aligned}
&\left(\frac{i}{\kappa}\nabla + h^{(0)}\mathbf{A}_N\right)^2 \psi_l^{(1)} - \psi_l^{(1)} = -\frac{\alpha}{\kappa^2}\frac{\partial\psi_l^{(0)}}{\partial\tau} - \psi_l^{(0)}\left|\psi_l^{(0)}\right|^2 \\
&-2h^{(1)}h^{(0)}\left|\mathbf{A}_N\right|^2\psi_l^{(0)} - 2h^{(1)}\frac{i}{\kappa}\left(\mathbf{A}_N\cdot\nabla\psi_l^{(0)}\right) - 2\frac{i}{\kappa}\left(\mathbf{a}_l^{(0)}\cdot\nabla\psi_l^{(0)}\right) \\
&-\frac{i}{\kappa}\psi_l^{(0)}\nabla\cdot\mathbf{a}_l^{(0)} - \frac{i}{\kappa}h^{(1)}\psi_l^{(0)}\nabla\cdot\mathbf{A}_N - 2h^{(0)}\psi_l^{(0)}\left(\mathbf{A}_N\cdot\mathbf{a}_l^{(0)}\right) \text{ in } \Omega, \qquad (105)
\end{aligned}$$

$$\begin{aligned}
\mathbf{n}\cdot\left((i/\kappa)\nabla + h^{(0)}\mathbf{A}_N\right)\psi_l^{(1)} + (i/D)\,\psi_l^{(1)} &= -\mathbf{n}\cdot\left(\mathbf{a}_l^{(0)} + h^{(1)}\mathbf{A}_N\right)\psi_l^{(0)} \\
&\quad \text{on } \partial\Omega. \qquad (106)
\end{aligned}$$

Substituting the expressions (101) for $\psi_l^{(0)}$ and (43) for $\mathbf{a}_l^{(0)}$ into (105) and (106) gives

$$
\begin{aligned}
&\left((i/\kappa)\,\nabla + h^{(0)}\mathbf{A}_N\right)^2 \psi_l^{(1)} - \psi_l^{(1)} = \\
&= e^{ih^{(0)}\kappa c y}\Big\{ -\frac{\alpha}{\kappa^2} f(-x)\frac{db}{d\tau} - b|b|^2 f^3(-x) - 2b|a|^2 f^2(x) f(-x) - 2b|a|^2 \frac{If(x)x}{4\kappa^2 c} \\
&\qquad\qquad - 2bh^{(0)}\,(x-c)\, f(-x)\left[h^{(1)}x + |a|^2 a_+ + |b|^2 a_-\right]\Big\} \\
&+ e^{-ih^{(0)}\kappa c y}\Big\{ -\frac{\alpha}{\kappa^2} f(x)\frac{da}{d\tau} - a|a|^2 f^3(x) - 2a|b|^2 f^2(-x) f(x) - 2a|b|^2 \frac{If(-x)x}{4\kappa^2 c} \\
&\qquad\qquad - 2ah^{(0)}\,(x+c)\, f(x)\left[h^{(1)}x + |a|^2 a_+ + |b|^2 a_-\right]\Big\} \\
&+ e^{3ih^{(0)}\kappa c y}\Big\{ -a^* b^2 f^2(-x) f(x) - 2a^* b^2 \frac{If(-x)}{4\kappa^2 c}\,(x-2c)\Big\} \\
&+ e^{-3ih^{(0)}\kappa c y}\Big\{ -b^* a^2 f^2(x) f(-x) - 2b^* a^2 \frac{If(x)}{4\kappa^2 c}\,(x+2c)\Big\}.
\end{aligned}
\tag{107}
$$

The solvability conditions are worked out in exactly the same way as before. We find

$$
S\frac{da}{d\tau} = a\left(P|a|^2 + Q|b|^2 + h^{(1)}R\right), \tag{108}
$$

$$
S\frac{db}{d\tau} = b\left(P|b|^2 + Q|a|^2 + h^{(1)}R\right), \tag{109}
$$

where P, Q, R are the same as in the time–independent case (cf. (50)–(52)) and

$$
S = \frac{\alpha}{\kappa^2}\int_{-d}^{d} f^2(x)dx. \tag{110}
$$

The initial conditions for the system (108), (109) at $\tau = 0$ are given by matching with the short–timescale solution (91) for $t \to \infty$. We get

$$
a(0) = C_{-1,0}, \qquad b(0) = C_{1,0}. \tag{111}
$$

3.3 Classification of Solutions

We will now classify the qualitative behaviour of the solutions of (108), (109) by means of a phase plane analysis.

Note that S is positive and that R can be written as

$$
R = -h^{(0)}\int_{-d}^{d} f^2(x)(x+c)^2 dx, \tag{112}
$$

where (52), (36) and (39) have been used. From (112) it follows that R is always negative. Therefore we define $r = Rh^{(1)}/S$, where r has the opposite sign to $h^{(1)}$.

Without loss of generality a and b can be taken as positive reals since if we set $a = |a|e^{i\varphi_1}$, $b = |b|e^{i\varphi_2}$ then equations (108), (109) imply $d\varphi_i/d\tau = 0$.

Furthermore, $a = b$ is a trajectory and interchanging $a(\tau)$ and $b(\tau)$ maps trajectories to trajectories. Thus, we only need to consider the sector $a \geq b$.

The fixed points of (108), (109) in the sector $a \geq b$ are just the solutions of the time–independent equations, namely the boundary state (53), the symmetric state (55) and the normal state, which corresponds to the origin $a = b = 0$.

We linearise about the fixed points (a_0, b_0) to obtain equations for $x = a - a_0$ and $y = b - b_0$. The linearised system at $(0, 0)$ reads

$$\begin{pmatrix} \dot{x} \\ \dot{y} \end{pmatrix} = r \begin{pmatrix} 1 & 0 \\ 0 & 1 \end{pmatrix} \begin{pmatrix} x \\ y \end{pmatrix}. \tag{113}$$

We find that the origin is an unstable node for $r > 0$ and a stable node for $r < 0$. For the boundary state, the Jacobian has the eigenvalues and eigenvectors

$$\lambda_1 = -2r, \qquad \mathbf{v}_1 = \begin{pmatrix} 1 \\ 0 \end{pmatrix}, \tag{114}$$

$$\lambda_2 = r\,\frac{P - Q}{P}, \qquad \mathbf{v}_2 = \begin{pmatrix} 0 \\ 1 \end{pmatrix}, \tag{115}$$

and for the symmetric state the eigenvalues and eigenvectors are

$$\lambda_1 = -2r, \qquad \mathbf{v}_1 = \begin{pmatrix} 1 \\ 1 \end{pmatrix}, \tag{116}$$

$$\lambda_2 = -2r\,\frac{P - Q}{P + Q}, \qquad \mathbf{v}_2 = \begin{pmatrix} 1 \\ -1 \end{pmatrix}. \tag{117}$$

The ratio $\gamma = b/a$ satisfies the equation

$$S\dot{\gamma} = \gamma(1 - |\gamma|^2)a^2(Q - P). \tag{118}$$

We are now in a position to classify the qualitative behaviour of the solutions of (108), (109).

For the case $r > 0$, the origin is an unstable node. The trajectories will therefore either approach one of the other fixed points or blow up. A complete classification is given in table 1. The sector numbers given in the first column refer to Figure 2 which summarises the table graphically. Figure 3 shows a typical phase plane in each case.

For $r < 0$ the origin is a stable node. The domain of attraction of the origin may be either finite or infinite. Again, we classify the possible solutions according to the presence of further fixed points in table 2. Sector numbers are as in Fig. 4. Typical phase planes are given in Fig. 5.

We refer to the case $P < 0$, $P + Q > 0$ as unrestricted boundary stability because solutions with sufficiently large b blow up, whereas solutions close to

	boundary state	symmetric state	remarks
$P > 0$, $P + Q > 0$ (sec. 1, 2, 8)	not present	not present	solutions blow up: "complete instability"
$P > 0$, $P + Q < 0$ (sec. 7)	not present	saddle with $\mathbf{v}_2$ unstable	blow–up with b/a tending to 0: "boundary instability"
$P < 0$, $P + Q > 0$ (sec. 3)	saddle with $\mathbf{v}_2$ unstable	not present	blow–up with b/a tending to 1: "symmetric instability"
$P < 0$, $Q < P$ (sec. 6)	stable node	saddle with $\mathbf{v}_2$ unstable	boundary state globally attracting.
$P < 0$, $P < Q < \|P\|$ (sec. 4, 5)	saddle with $\mathbf{v}_2$ unstable	stable node	symmetric state globally attracting.

Table 1: Classification of the long–timescale solutions for the case $r > 0$.

$b = 0$ decay to zero. Similarly, for $P > 0$, $P + Q < 0$, solutions near $a = b$ decay, whereas all other solutions blow up. In both cases, the trajectory approaching the saddle point in the direction of the stable eigenspace separates the sector $a \geq b$ into two unbounded regions containing decaying solutions and solutions which blow up in finite time (cf. phase planes (3) and (4) in Fig. 5).

In the cases of restricted stability, the trajectory approaching the saddle point in direction of the stable eigenspace originates at the unstable node and thereby separates the sector $a \geq b$ into a bounded region of decaying solutions and an unbounded region of "exploding" solutions (cf. phase planes (5) and (6) in Fig. 5).

Let us attempt to interpret these results physically. We divide the sectors in diagrams 2 and 4 into those that exhibit the same qualitative behaviour as bulk type I materials, namely sectors 1,2,3,7 and 8, and those that exhibit the same qualitative behaviour as bulk type II materials, namely sectors 4,5 and 6.

Sectors 1,2,3,7,8: Type I behaviour

1. $h^{(1)} > 0$: Here the normal state ($a = b = 0$) is linearly stable. The domain of attraction of the normal state can be either

   (a) finite for sectors 1, 2, 8 in diagram 4 (cf. planes (5) and (6) in Fig. 5),

   (b) infinite along $a = b$ for sector 3 in diagram 4 (cf. plane (4) in Fig. 5)

	boundary state	symmetric state	remarks
$P < 0$, $P + Q < 0$ (sec. 4, 5, 6)	not present	not present	"complete stability"
$P < 0$, $P + Q > 0$ (sec. 3)	not present	saddle with $\mathbf{v}_1$ unstable	domain of attraction infinite along $b = 0$: "unrestricted boundary stability"
$P > 0$, $P + Q < 0$ (sec. 7)	saddle with $\mathbf{v}_1$ unstable	not present	domain of attraction infinite along $a = b$: "unrestricted symmetric stability"
$P > 0$, $Q > P$ (sec. 2)	unstable node	saddle with $\mathbf{v}_1$ unstable	finite domain of attraction: "restricted symmetric stability" (b/a increasing)
$P > 0$, $-P < Q < P$ (sec. 1, 8)	saddle with $\mathbf{v}_1$ unstable	unstable node	finite domain of attraction: "restricted boundary stability" (b/a decreasing)

Table 2: Classification of the long–timescale solutions for the case $r < 0$.

(c) infinite along the boundary $a \neq 0$, $b = 0$ (and vice versa) for sector 7 in diagram 4 (cf. plane (3) in Fig. 5)

For (a) any large perturbation will lead to instability. Two types of instability are possible. For sector 2 the phase boundaries sweep in from both sides since $b \to a$ as the solutions blow up. In sectors 1 and 8 we have phase boundaries sweeping in from a single side.

For (b) a perturbation that is equal at both boundaries will be stable, but a perturbation localised at a single side will be unstable. The instability will have a phase boundary sweeping across the film from one side.

For (c) a perturbation localised at one boundary will be stable, but a perturbation including both boundaries will lead to instability. The instability will have phase boundaries sweeping in from both sides.

2. $h^{(1)} < 0$: Here the normal state is linearly unstable. Hence, all solutions blow up. There are again three types of behaviour.

(a) For sectors 1, 2, 8 in diagram 2 the behaviour of the phase boundaries sweeping in depends on the initial conditions (complete instability).

(b) For sector 3 in diagram 2 the phase boundaries sweep in from both sides (symmetric instability, cf. plane (4) in Fig. 3).

(c) For sector 7 in diagram 2 the phase boundaries always sweep in from one side only (boundary instability, (cf. plane (3) in Fig. 5).

Sectors 4,5,6: Type II behaviour

1. $h^{(1)} > 0$: The normal state is both linearly and non–linearly stable (complete stability). All solutions decay to zero (sectors 4, 5, 6 in diagram 4, cf. planes (1) and (2) in Fig. 5).

2. $h^{(1)} < 0$: The normal state is linearly unstable and the superconducting state is stable. There are two possible superconducting solutions and two corresponding types of behaviour.

   (a) All perturbations tend to the symmetric superconducting state (sectors 4, 5 in diagram 2, cf. plane (6) in Fig. 3).

   (b) All perturbations tend to a boundary superconducting state (sector 6 in diagram 2, cf. plane (5) in Fig. 3).

3.4 Numerical Results

We are now in a position to classify the solution for given values of P and Q, which in turn depend on the solution f of the eigenvalue problem (35), (37). It is of interest to determine which sectors in diagrams 2 and 4 are reached for different values of the parameters d, κ and D.

In the following we will not attempt to deal with the full problem but consider the special case $D = \infty$ only. For this case (corresponding to a superconducting film adjacent to an insulator) we have performed numerical computations of the coefficients P and Q as functions of κd and d, which are a natural choice once we scale the eigenvalue problem onto a fixed domain by setting $x = Xd$. We get

$$\frac{1}{(\kappa d)^2} f_{XX} + f - (h^{(0)}d)^2 (X + \tilde{c})^2 f = 0, \tag{119}$$

$$f_X(-1) = 0, \quad f_X(1) = 0, \tag{120}$$

where

$$\tilde{c} = c/d. \tag{121}$$

Equations (119), (120) represent a Sturm–Liouville system. The general form of this problem reads

$$\frac{d}{dx}\left(p(x)\frac{df}{dx}\right) + (\lambda\rho(x) - q(x))f = 0, \tag{122}$$

$$a_1 f(-1) + a_2 p(-1) f'(-1) = 0, \quad b_1 f(1) + b_2 p(1) f'(1) = 0 \tag{123}$$

where λ is the eigenvalue. The function $p(x)$ is positive and continuously differentiable, and ρ is positive and $\rho(x)$ and $q(x)$ are continuous on (-1,1). The system (122), (123) has an infinite sequence $\lambda_0 < \lambda_1 < \lambda_2 < \ldots$ of eigenvalues with $\lambda_n \to \infty$ as $n \to \infty$ [1]. Since the sequence $\{\lambda_n\}_{n=0}^{\infty}$ of eigenvalues grows without bound, there can only be a finite number of negative eigenvalues λ_n. Consequently, there is only a finite number of bifurcation values for $h^{(0)}$ (a positive λ_n would correspond to an imaginary $h^{(0)}$). The lowest eigenvalue $\lambda_0 < 0$ gives the highest value of the magnetic field $h^{(0)}$.

Since the eigenvalues depend on $\tilde{c}$ we have to adjust $\tilde{c}$ so that $\lambda_0(\tilde{c})$ is minimal. The minimum of $\lambda_0(\tilde{c})$ lies in $(-1, 1)$ because of the condition (39), which can only be satisfied by $f \equiv 0$ for $|c| \geq 1$. For uniqueness we take $\tilde{c} > 0$. We solve the Sturm–Liouville Problem for a given value of $\tilde{c}$ by a phase function method provided in the NAG–library [14, 1], and minimise the eigenvalue by means of the “golden section search” algorithm [16].

After putting $x = Xd$, we can write the functions P and Q as

$$P = d(F_s + d^2 H_s), \quad Q = d(F_a + d^2 H_a), \tag{124}$$

with functions

$$F_s(\kappa d) = -\int_{-1}^{1} f^4(X)dX, \tag{125}$$

$$F_a(\kappa d) = -2\int_{-1}^{1} f^2(X)f^2(-X)dX, \tag{126}$$

$$H_s(\kappa d) = 2|\lambda_0|\int_{-1}^{1} (g(X))^2\, dX, \tag{127}$$

$$H_a(\kappa d) = 2\int_{-1}^{1}\left[|\lambda_0| g(X)g(-X) + \frac{p^2 J^2}{|\lambda_0|\,(4\tilde{c})^2}\right] dX. \tag{128}$$

The functions $g(X)$ and $J(X)$ are defined by

$$g(X) = \int_{-1}^{X} f^2(u)(u + \tilde{c})du, \tag{129}$$

$$J(X) = f(X)f_X(-X) + f(-X)f_X(X), \tag{130}$$

and are analogous to (36) and (45).

Before turning to the results for F_s, F_a, H_s and H_a let us first look at $f(X)$ and the decrease $g(X)$ of the magnetic field inside the film. For comparison, they are also plotted for $c = 0$.

Fig. 6 ,7 and 8, 9 show two extreme cases. For the small value $1/(\kappa d) = 0.2$ the order parameter is non–zero in a small region near the boundary for the asymmetric solution and near the middle of the interval for the symmetric solution with $\tilde{c} = 0$. Since $1/(\kappa d)^2$ multiplies the second derivative in equation (119), the parameter $1/(\kappa d)$ gives the lengthscale for an $O(1)$–change in f. If $1/(\kappa d) \ll 1$ we can therefore expect that the film is superconducting in a small region of size $1/(\kappa d)$ only.

If $1/(\kappa d)$ is not small compared with 1, the superconducting state cannot be confined to the boundary or the central region, but must spread out over the whole film. Eventually, for $1/(\kappa d) \gg 1$ the solution becomes effectively constant since there is not enough space in the interval for a significant change in f. We then expect the symmetric solution to be valid since it requires the least variation in f over $[-1, 1]$ to satisfy the boundary conditions. In between, for $1/(\kappa d)_c \approx 1.103$ the asymmetric solution ceases to exist.

These observations can be applied to the ratio of the lowest eigenvalue $\lambda_0(c_{min}/d) = -(h^{(0)}d)^2$ to the eigenvalue $\lambda_0(0)$ of the symmetric solution, given in Fig. 10.

For $1/(\kappa d) \to 0$ the ratio tends to $\approx 1.7^2 = 2.89$, because the critical field for the half–space solution is given by $h^{(0)} \approx 1.7\kappa$, whereas it is $h^{(0)} = \kappa$ for the infinite domain [3]. Clearly, the eigenvalues will come closer for increasing $1/(\kappa d)$, and finally the ratio must tend to 1 as the critical value $1/(\kappa d)_c$ is approached.

The half–space solution also explains the linear dependence of $\tilde{c}$ on $1/(\kappa d)$ for not too large values of $1/(\kappa d)$ (shown in Fig. 11): for the half–space solution in the domain $x > 0$, we have $c = 1/h^{(0)}$ for $D = \infty$ [3]. If we approximate the film by a halfspace centred on the plane $x = -d$ the corresponding quantity is $d(1 - \tilde{c})$, giving $d(1 - \tilde{c}) = 1/h^{(0)}$. Using (121) and $h^{(0)} \approx 1.7\kappa$ for the half–space solution we get

$$1 - \tilde{c} = \frac{1}{1.7\kappa d}. \tag{131}$$

The behaviour of the functions F_s, H_s and F_a, H_a shown in Fig 12 and 13 is now obvious from our previous discussion. Clearly, $|F_s|$ must be decreasing since f "spreads out" as as $1/(\kappa d)$ increases. However, this does not apply to H_s, since g is given by an integral of $f^2(u)$ multiplied by $(u + \tilde{c})$, which is small in the region where f is large. As f is "spread out", the effect of the factor $(u + \tilde{c})$ is reduced. The functions F_a and H_a are very small for small $1/(\kappa d)$ since in this case there is very little overlap of $f(X)$ and $f(-X)$.

As $1/(\kappa d) \to 1/(\kappa d)_c$, the eigenfunctions $f(X)$ and $f(-X)$ become identical and $\tilde{c} \to 0$. Therefore $J = 0$ by (130) and consequently $H_a = 2H_s$ and $F_a = 2F_s$.

We are now in a position to determine the possible types of solutions according to our classification above. Changes in the type of solution are associated with the crossing of a sector boundary in the diagrams 2 and 4. These sector boundaries are given by the equations

$$P = 0, \quad Q = 0, \quad P + Q = 0, \quad P - Q = 0, \tag{132}$$

or, in terms of F_s, H_s and F_a, H_a

$$P = d\left[F_s\left(\frac{1}{\kappa d}\right) + d^2 H_s\left(\frac{1}{\kappa d}\right)\right] = 0, \tag{133}$$

$$Q = d\left[F_a\left(\frac{1}{\kappa d}\right) + d^2 H_a\left(\frac{1}{\kappa d}\right)\right] = 0, \tag{134}$$

$$P + Q = d\left[(F_s + F_a)\left(\frac{1}{\kappa d}\right) + d^2\left(H_s + H_a\right)\left(\frac{1}{\kappa d}\right)\right] = 0, \tag{135}$$

$$P - Q = d\left[(F_s - F_a)\left(\frac{1}{\kappa d}\right) + d^2\left(H_s - H_a\right)\left(\frac{1}{\kappa d}\right)\right] = 0. \tag{136}$$

Solutions to these equations are curves in the $(1/(\kappa d), d)$–plane, shown in Fig. 14

The curves separate the $(1/(\kappa d), d)$–plane into different regions. In each of these regions the functions P, Q, $P + Q$ and $P - Q$ do not change sign, and we can associate them with sectors in the diagrams 2 and 4. We find regions corresponding to sectors 1, 2, 3, 4, 5 and 6. We note in particular the existence of a region corresponding to sector 6, that is, to the stable boundary states for $h^{(1)} < 0$. This is in contrast to Kulik [12], who came to the conclusion that such a region could not exist.

We cannot completely rule out the possibility of a crossing of the curves $P = 0$ and $Q = 0$ for small values of $1/(\kappa d)$, which would give sectors 7 and 8, too. For small $1/(\kappa d)$ however, the existence of the behaviour corresponding to sector 7 seems unlikely. For a magnetic field $h^{(1)} < 0$ it implies that a nearly symmetric perturbation must tend to one side or the other. But if $1/(\kappa d)$ is small, the film is thick, and the solutions at both sides should not interfere with each other.

4 Conclusion

We have examined the bifurcation of a slab of superconducting material from the normal state to a superconducting state as the applied magnetic field h is decreased. The largest eigenvalue defines the critical magnetic field, which is known as h_{c_3}, and is a double eigenvalue in this case, which results in a rich variety of possible behaviour.

Providing the thickness of the film $2d$ is not too large, there are three nontrivial superconducting solutions, corresponding to a superconducting region localised near each edge of the film, and at both edges respectively. This last solution has a row of superconducting vortices down the centre of the slab.

We have classified the behaviour of the superconductor for a wide range of values of the Ginzburg-Landau parameter κ and the thickness $2d$, for the case when the adjacent material is an insulator. We find that the response can be identified as qualitatively similar to bulk type I or bulk type II behaviour.

For bulk type II behaviour the normal state is linearly and weakly nonlinearly stable when $h > h_{c_3}$. For $h < h_{c_3}$ we found that either the boundary superconducting state or the symmetric superconducting state would be globally attracting, and there are regions of parameter space corresponding to each case. This last result is in contrast to Kulik [12], who precluded the existence of stable boundary states.

For bulk type I behaviour we found that for $h < h_{c_3}$ the solution would blow up, corresponding to an initiation of phase boundaries separating wholly superconducting material form normal material sweeping through the material. For $h > h_{c_3}$ the normal state is linearly stable, but nonlinearly unstable. There are regions of parameter space for which the domain of attraction of the normal state is finite, and regions where it is infinite.

References

[1] Birkhoff, G. and Rota, G.-C., Ordinary Differential Equations. 4th edition, Wiley (1989).

[2] Bolley, C. & Helffer, B., "Rigorous results on Ginzburg-Landau models in a film submitted to an exterior parallel magnetic field". Preprint Ecole centrale de Nantes, (1993).

[3] Chapman, S. J., Nucleation of Superconductivity in Decreasing Fields I. European Journal of Applied Mathematics, **5**, 4, 449 (1994).

[4] Chapman, S. J., Nucleation of Superconductivity in Decreasing Fields II. European Journal of Applied Mathematics, **5**, 4, 469 (1994).

[5] Chapman, S. J., Howison, S. D. & Ockendon, J. R., Macroscopic Models of Superconductivity. *SIAM Review*, **34**, 4, 529-560 (1992).

[6] Courant, R. and Hilbert, D., Methods of Mathematical Physics I. Interscience, New York (1953).

[7] Fink, H. J., Vortex Nucleation in a Superconducting Slab near a Second-Order Phase Transition and Excited States of the Sheath near H_{c_3}, *Phys. Rev.*, **177**, 2, 732-737 (1969).

[8] De Gennes, P. G., Superconductivity of Metals and Alloys. Benjamin, New York (1966).

[9] Du, Q., Gunzburger, M. D. and Peterson, J., Analysis and Approximation of the Ginzburg–Landau Model of Superconductivity, *SIAM Review* **34**, 1, 54–81 (1992).

[10] Ginzburg, V. L. & Landau, L. D., On the Theory of Superconductivity. *J.E.T.P.* **20**, 1064 (1950).

[11] Gor'kov, L. P. and Eliashberg, G. M., Generalisation of the Ginzburg–Landau equations for non–stationary problems in the case of alloys with paramagnetic impurities. *Soviet Physics J.E.T.P.* **27**, 328 (1968).

[12] Kulik, I. O., Vortex Structure in Superconducting Films in a Parallel Field. *Soviet Physics J.E.T.P.* **25**, 6, 1085 (1967).

[13] Millman, M. H. and Keller, J. B., Perturbation Theory of Nonlinear Boundary–Value Problems, *J. Math. Phys.* **10**, 2, 342 (1969).

[14] NAG Fortran Library Manual, Mark 16, Volume 2, Chapter D02.

[15] Odeh, F., Existence and Bifurcation Theorems for the Ginzburg-Landau Equations. *J. Math. Phys.* **8**, 12, 2351 (1967).

[16] Press, W. H., Flannery, B. P., Teukolsky, S. A. and Vetterling, W. T., Numerical Recipes, Cambridge University Press (1989).

[17] Saint–James, D. and De Gennes, P. G., *Phys. Lett.* **7**, 306 (1963).

[18] Schultens, H. A., Current Vortices in Superconducting Films at the Surface Parallel Critical Field. *Z. Phys.* **232**, 430 (1970).

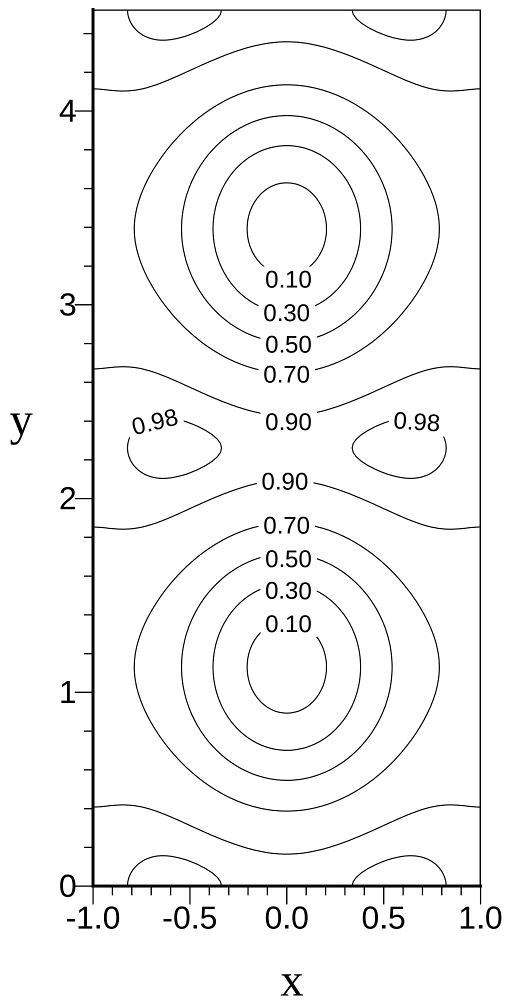

Figure 1: Contour lines of $|\psi^{(0)}|^2$ for the symmetric state $(1/\kappa d = 0.8)$.

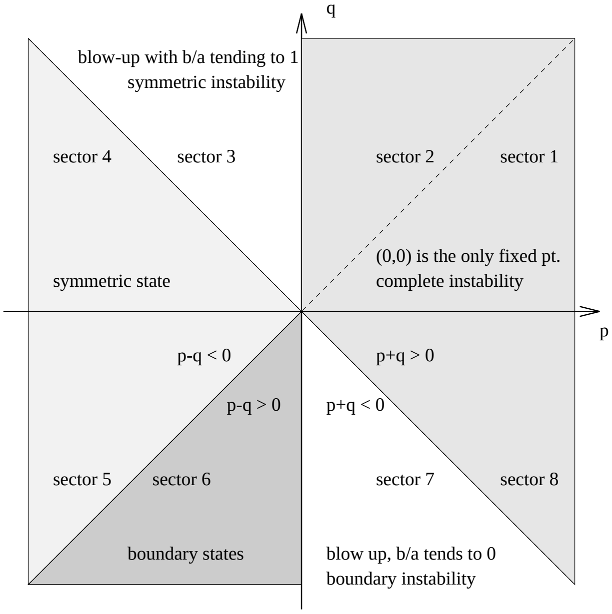

Figure 2: Overview of the solutions to the long-timescale equations for positive r, i.e. magnetic field below critical value.

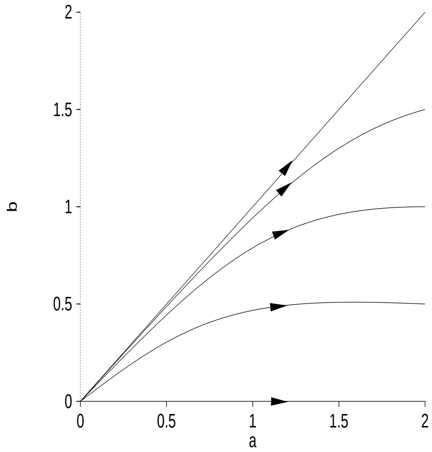

(1) : P=1, Q=-0.5 (sector 8)

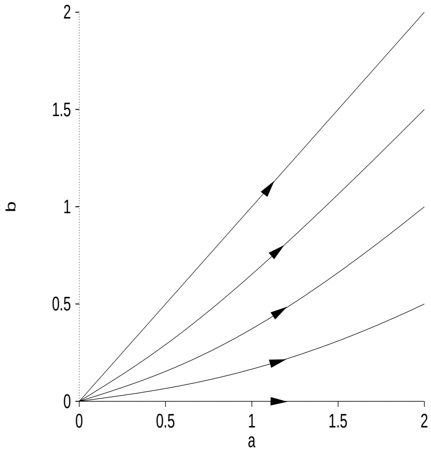

(2): P=1, Q=2 (sector 2)

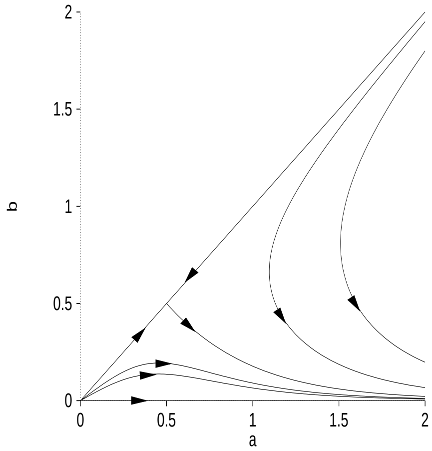

(3): P=1, Q=-5 (sector 7)

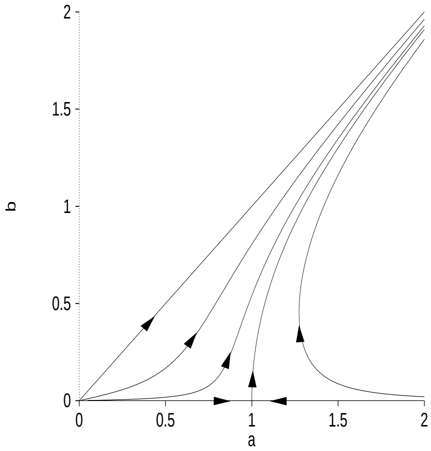

(4): P=-1, Q=3 (sector 3)

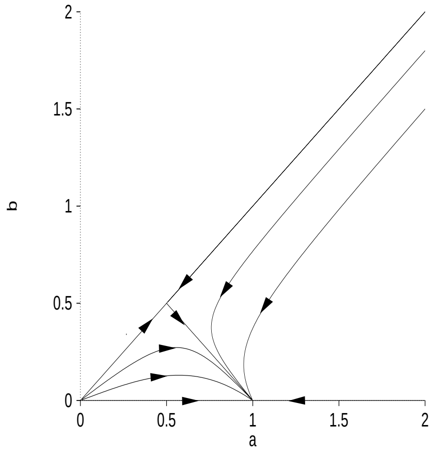

(5): P=-1, Q=-3 (sector 6)

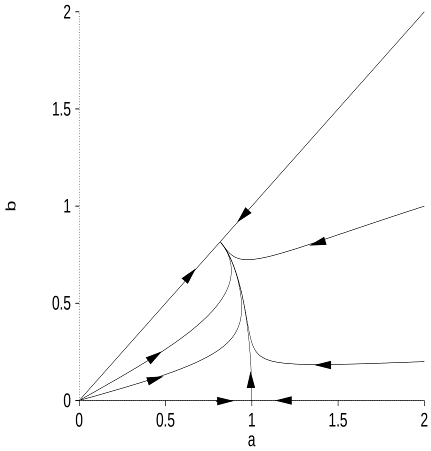

(6): P=-1, Q=-0.5 (sector 5)

Figure 3: Phase planes for $r = 1$.

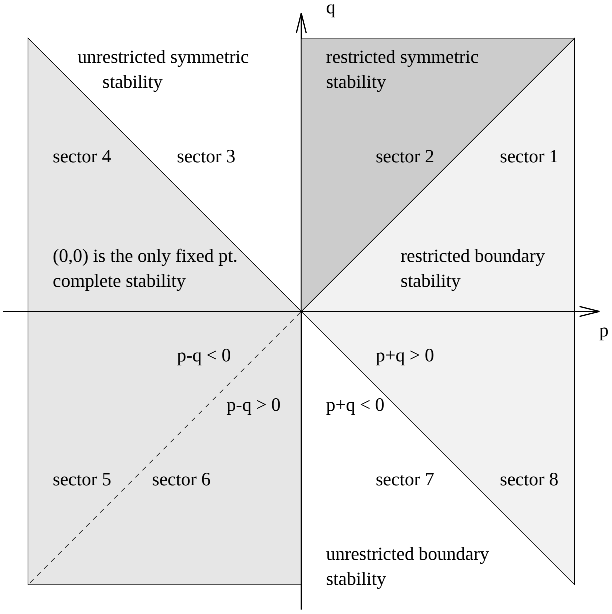

Figure 4: Overview of the solutions to the long-timescale equations for negative r, i.e. magnetic field above critical value.

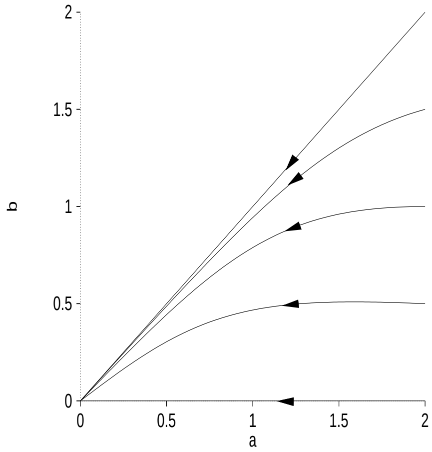

(1) : P=-1, Q=0.5 (sector 4)

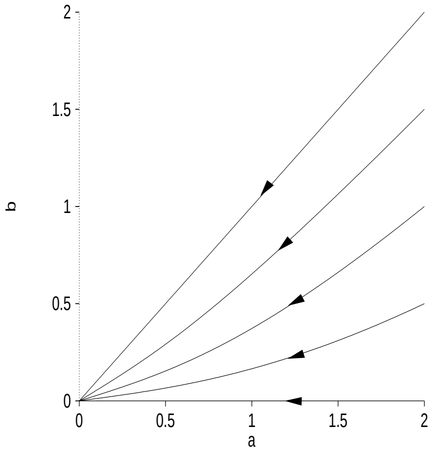

(2): P=-1, Q=-2 (sector 6)

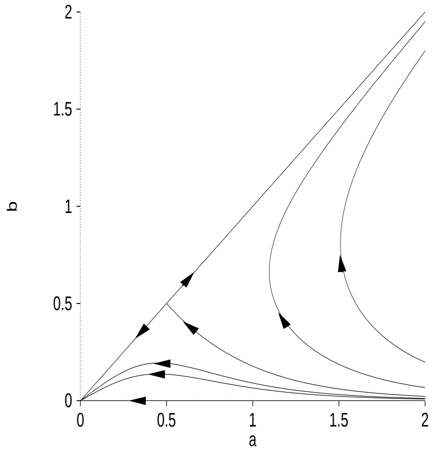

(3): P=-1, Q=5 (sector 3)

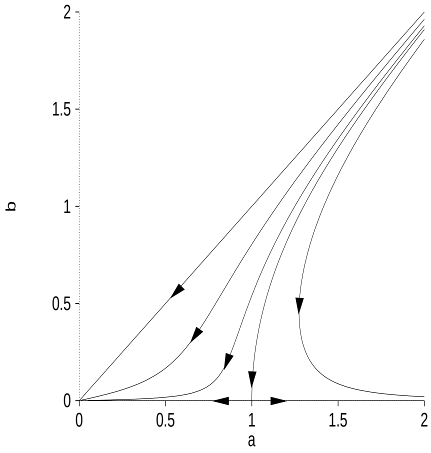

(4): P=1, Q=-3 (sector 7)

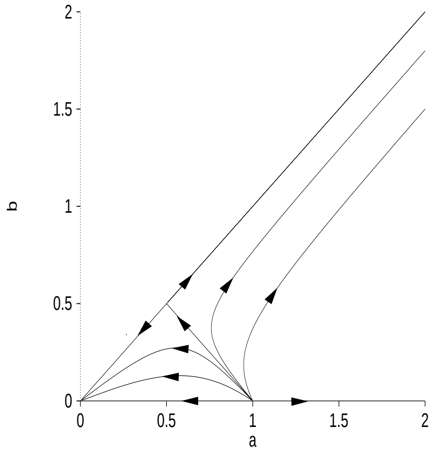

(5): P=1, Q=3 (sector 2)

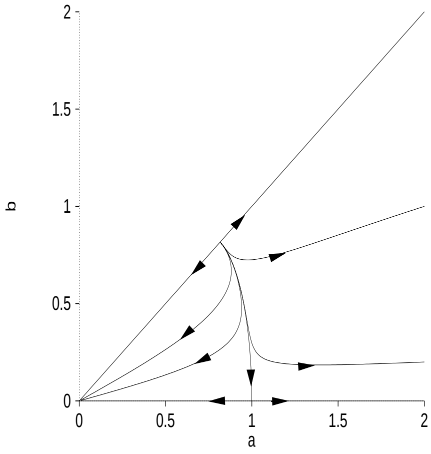

(6): P=1, Q=0.5 (sector 1)

Figure 5: Phase planes for $r = -1$.

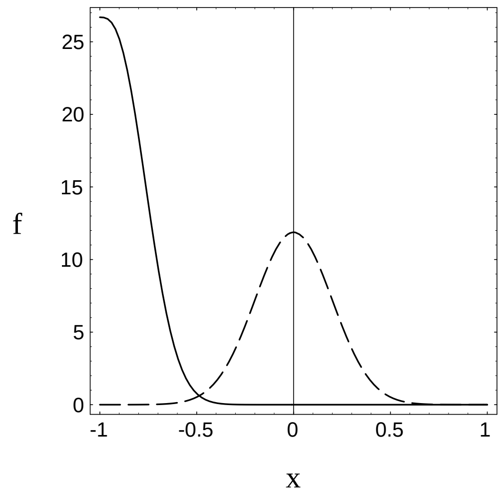

Figure 6: Eigenfunctions $f(X)$ for $c = c_{min}$ and $c = 0$ (dashed), $1/(\kappa d) = 0.2$.

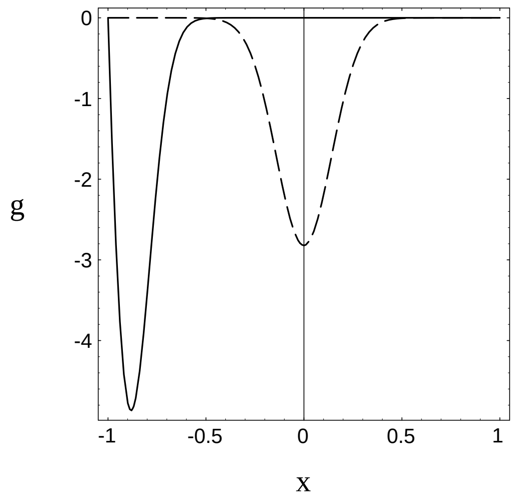

Figure 7: Decrease g of the magnetic field for c_{min} and $c = 0$ (dashed), $1/\kappa d = 0.2$.

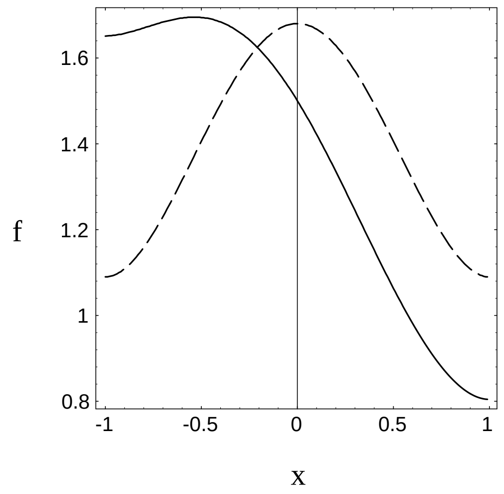

Figure 8: Eigenfunctions $f(X)$ for $c = c_{min}$ and $c = 0$ (dashed), $1/(\kappa d) = 1.05$.

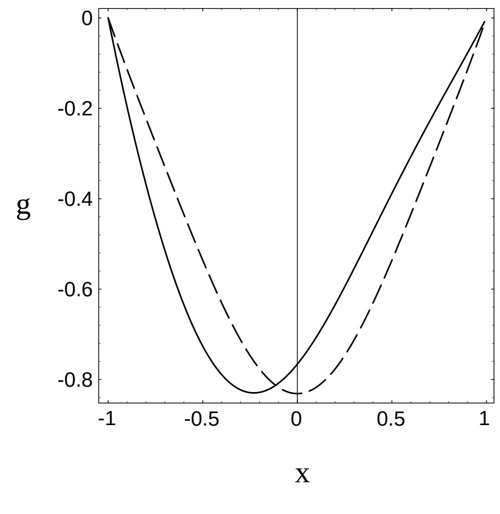

Figure 9: Decrease g of the magnetic field for c_{min} and $c = 0$ (dashed), $1/\kappa d = 1.05$.

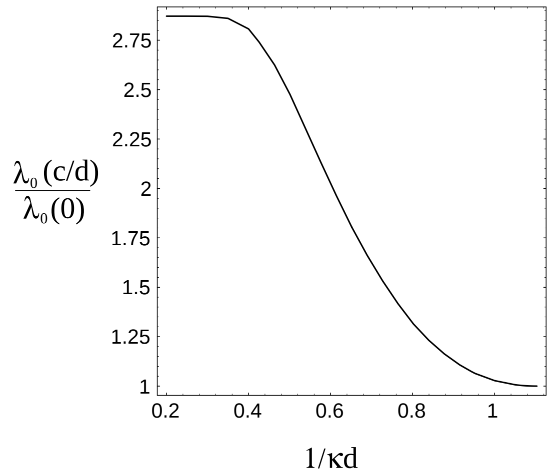

Figure 10: Ratio of the eigenvalues λ_0 for $c/d = \tilde{c}_{min}$ and $c = 0$ as function of $1/\kappa d$.

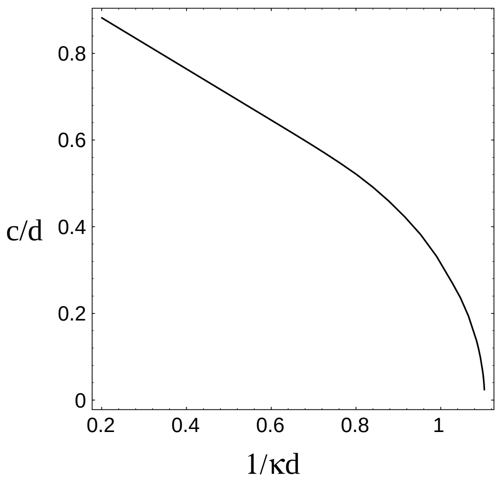

Figure 11: The asymmetry parameter c/d as function of $1/\kappa d$.

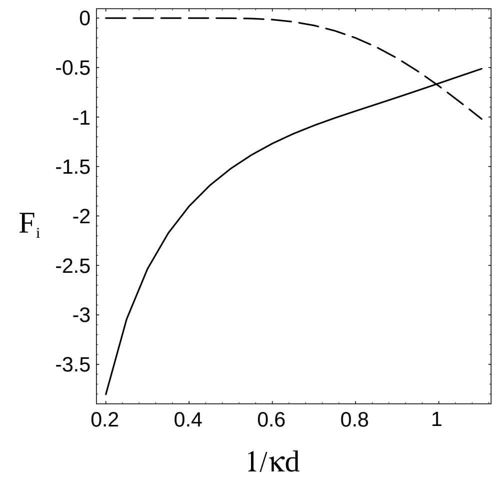

Figure 12: F_s and F_a (dashed) as functions of $1/\kappa d$.

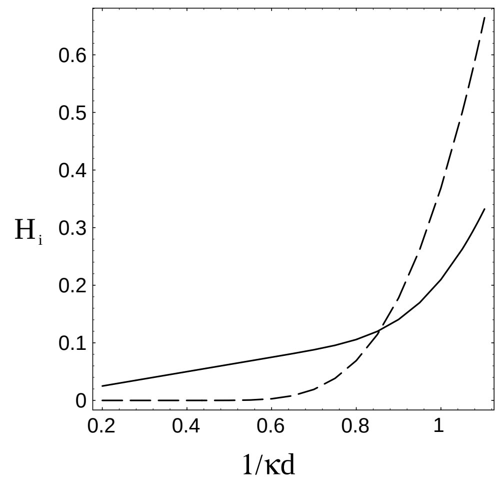

Figure 13: H_s and H_a (dashed) as functions of $1/\kappa d$.

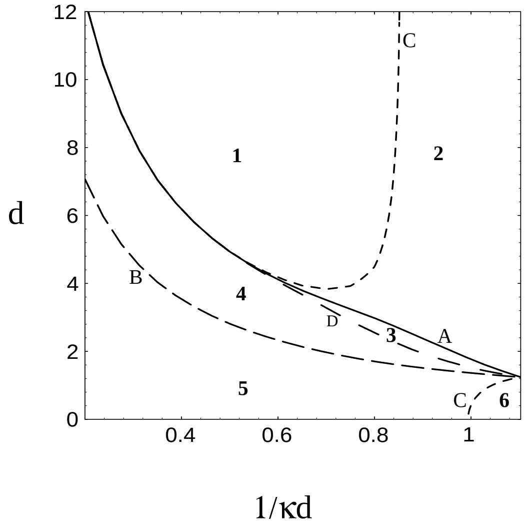

Figure 14: The curves $P = 0$ (A), $Q = 0$ (B), $P + Q = 0$ (C), $P - Q = 0$ (D) and the sector numbers **1** - **6** in the $(1/\kappa d,\, d)$–plane.